Research Paper

Osthole resensitizes CD133+ hepatocellular carcinoma cells to cisplatin treatment via PTEN/AKT pathway

Junfeng Ye[1], Di Sun[2], Ying Yu[1], Jinhai Yu[3]

[1]Department of Hepato-Biliary-Pancreatic Surgery, First Hospital Jilin University, Changchun 130021, Jilin Province, China
[2]Department of Colorectal and Anal Surgery, First Hospital Jilin University, Changchun 130021, Jilin Province, China
[3]Department of Gastrointestinal Surgery, First Hospital Jilin University, Changchun 130021, Jilin Province, China

Correspondence to: Jinhai Yu; **email:** jilinfangfang@yeah.net
Keywords: osthole, PTEN, AKT, Bcl-2, cisplatin
Received: February 28, 2020 **Accepted:** May 27, 2020 **Published:** July 16, 2020

ABSTRACT

The population of CD133 positive cancer cells has been reported to be responsible for drug resistance **of hepatocellular carcinoma (HCC). However, the potential molecular mechanism by which CD133+ HCC cells develop drug resistance is still unclear. In this study, we found that CD133+ HepG2 and Huh7 cells were resistant to cisplatin treatment, compared to the CD133- HepG2 and Huh7 cells. However, treatment with osthole, a natural coumarin isolated from umbelliferae plant monomers, was found to resensitize CD133+ HepG2 and Huh7 cells to cisplatin treatment. In the mechanism research, we found that treatment with osthole increased the expression of PTEN. As a result, osthole inhibited the phosphorylation of AKT and Bad to decrease the amount of free Bcl-2 in CD133+ HepG2 and Huh7 cells. Finally, cisplatin-induced mitochondrial apoptosis was expanded. In conclusion, combination treatment with osthole can resensitize CD133+ HCC cells to cisplatin treatment via the PTEN/AKT pathway.**

INTRODUCTION

Hepatocellular carcinoma (HCC) is one of the most common and lethal human malignant cancers worldwide [1, 2]. Although surgery treatment is the most effective treatment strategy for the early stage of HCC, tumors in many HCC patients are unresectable because they are usually diagnosed in an advanced stage. For these patients, the systematic chemotherapy and immunotherapy are irreplaceable and valuable [3–6]. Unfortunately, cancer cells usually develop mechanisms to acquire the resistance against anti-tumor drugs [7, 8]. Recently, studies demonstrate that drug resistance is partially induced by a population of CD133 positive cells in some cancers including HCC [9–11].

CD133 is a glycoprotein on cell surface. Previous studies have indicated that cancer cells which express CD133 exhibit "stem-like", and thus they are called "cancer stem cells" [12–14]. These CD133 positive cancer cells have high self-renewal capacity and multilineage differentiation potential. They are important for tumor formation and development [15, 16]. Furthermore, studies indicate that CD133 positive cells are responsible for the high resistance to chemo-therapeutic drugs [17, 18]. This population of cancer cells may represent a novel target for improving the chemotherapy.

Previous studies have proved that some natural plants are a significant source of potential drugs against cancer. Among these natural drugs, osthole has been reported to inhibit the growth of some cancers [19–21]. Osthole is a natural coumarin that is isolated from *Cnidium monnieri*. Its chemical formula is $C_{15}H_{16}O_3$. Studies indicate that osthole exerts a wide variety of biological effects

including anti-seizure, anti-osteoporosis and anti-inflammation [22–24]. More importantly, studies have found that osthole can partially inhibit the epithelial-mesenchymal transition process and induce apoptosis or cell cycle arrest in some cancers [25, 26]. However, little is known regarding to the effect of osthole on the chemoresistance of HCC. The aim of this study is to explore the effect of osthole on cisplatin treatment against $CD133^+$ HCC cells which are chemoresistant.

RESULTS

CD133 positive HCC cells were resistant to cisplatin

We first separated CD133 positive and negative population in Huh7 and HepG2 cell lines, the purity of these two populations was detected by flow cytometry (Figure 1A). Under the treatment of cisplatin with equal concentrations, we found significant resistance in $CD133^+$ Huh7 and HepG2 cells compared to the $CD133^-$ Huh7 and HepG2 cells (P<0.05) (Figure 1B). We confirmed that IC50 of cisplatin to $CD133^+$ Huh7 cells was 4.64 fold higher than that to $CD133^-$ Huh7 cells (P<0.05). Meanwhile, IC50 of cisplatin to $CD133^+$ HepG2 cells was 5.32 fold higher than that to $CD133^-$ HepG2 cells (P<0.05) (Figure 1C). We demonstrated that CD133 positive HCC cells were resistant to cisplatin.

Downregulation of PTEN is responsible for the cisplatin resistance of $CD133^+$ HCC cells

Results of western blot analysis showed that expression of PTEN was significantly lower in $CD133^+$ Huh7 and HepG2 cells compared to the $CD133^-$ Huh7 and HepG2 cells (P<0.05) (Figure 2A). To explore whether the CD133 positive HCC cells exhibited significant cisplatin resistance was associated with downregulation of PTEN, we compulsively expressed the PTEN in $CD133^+$ Huh7

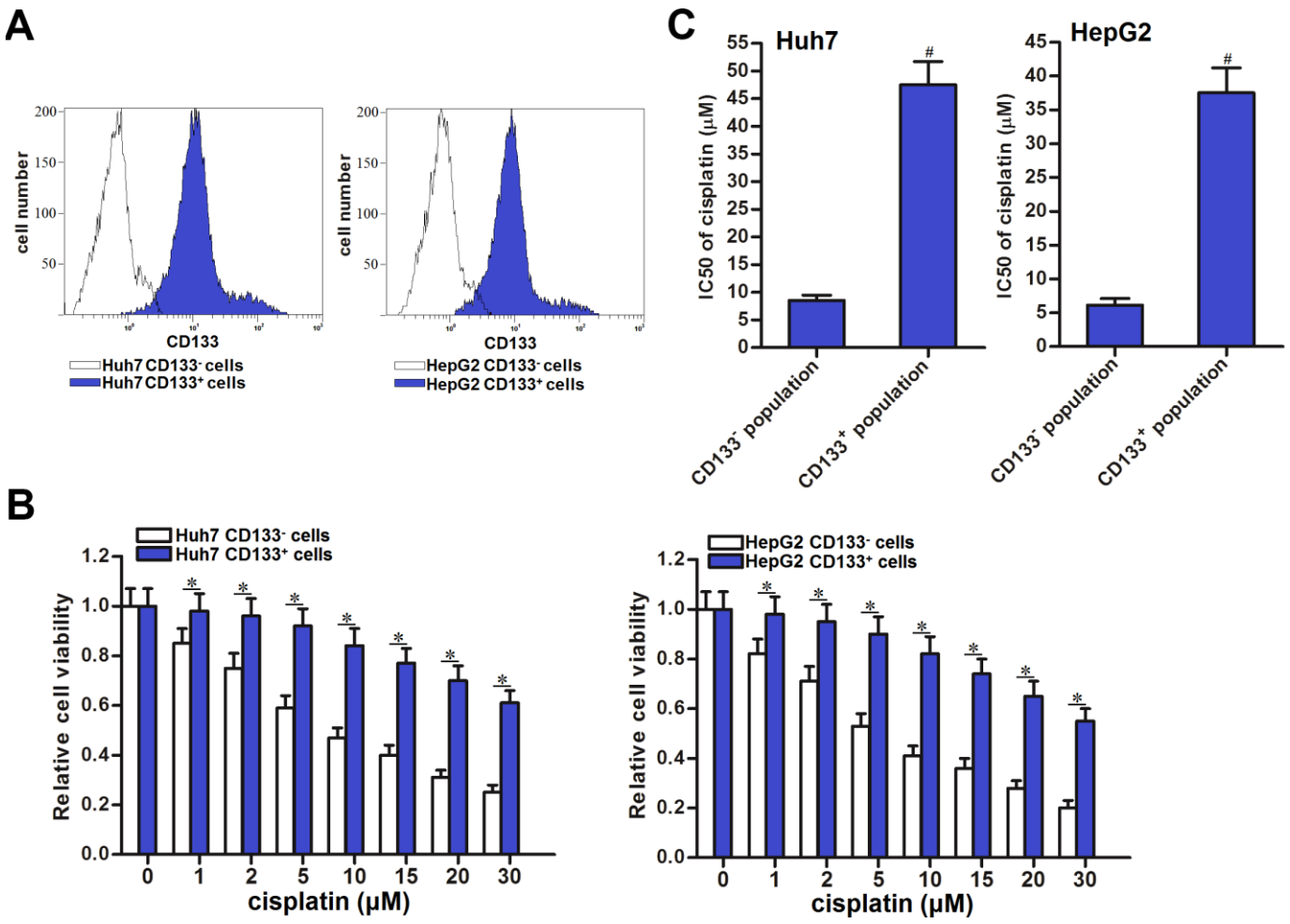

Figure 1. Cisplatin resistance of $CD133^+$ HCC cells. (**A**) Purity of sorted $CD133^+$ and $CD133^-$ Huh7 and HepG2 cells was tested by flow cytometry. (**B**) Sensitization of $CD133^+$ and $CD133^-$ Huh7 and HepG2 cells to different concentrations of cisplatin (0~30 μM). *P<0.05. (**C**) IC50 of cisplatin to $CD133^+$ and $CD133^-$ Huh7 and HepG2 cells. #P<0.05 *vs.* $CD133^-$ population.

and HepG2 cells by using PTEN eukaryotic expression plasmid (Figure 2B). We then found that recovery of PTEN expression in $CD133^+$ Huh7 and HepG2 cells increased their sensitivity to cisplatin treatment ($P<0.05$) (Figure 2C). On the other hand, we performed a loss-of-function test on PTEN by using PTEN specific siRNA in $CD133^-$ Huh7 and HepG2 cells (Figure 2D). We then found that knockdown of PTEN induced significant cisplatin resistance in $CD133^-$ Huh7 and HepG2 cells ($P<0.05$) (Figure 2E). These data indicated that PTEN expression partially determined the sensitivity of cisplatin to HCC. Downregulation of PTEN is responsible for the cisplatin resistance of CD133 positive HCC cells.

Osthole decreased the cisplatin resistance of CD133 positive HCC cells

To explore whether the osthole affected the chemo-resistance of CD133 positive HCC cells, we co-treated the $CD133^+$ Huh7 and HepG2 cells with cisplatin and osthole. Comparing to the cisplatin single treatment groups, combination treatment groups with cisplatin and osthole showed lower cell viability ($P<0.05$) (Figure 3A). We confirmed that osthole decreased the IC50 of cisplatin by 84.3% to $CD133^+$ Huh7 cells and 80.5% to $CD133^+$ HepG2 cells ($P<0.05$) (Figure 3B). Furthermore, we calculated that combination index (CI) with cisplatin and osthole was greater than 1.15 in $CD133^+$ Huh7 cells (Table 1) and $CD133^+$ HepG2 cells (Table 2). These data demonstrated that osthole exhibited synergistic effect on cisplatin. On the other hand, we tested the effect of osthole on the $CD133^-$ HCC cells. We found that osthole decreased the IC50 of cisplatin by 47.5% to $CD133^-$ Huh7 cells and 40.7% to $CD133^-$ HepG2 cells ($P<0.05$) (Figure 3C). These data indicated that $CD133^+$ HCC cells are more sensitive to osthole than the $CD133^-$ HCC cells. Treatment with osthole can decrease the cisplatin resistance of CD133 positive HCC cells.

Osthole partially reversed the cisplatin resistance of CD133 positive HCC cells through upregulation of PTEN

Results of qRT-PCR and western blot analysis showed that osthole treatment can increase the expression of PTEN at the mRNA level (Figure 4A) and the protein level (Figure 4B) in $CD133^+$ Huh7 and HepG2 cells. To investigate whether the osthole resensitized CD133 positive HCC cells to cisplatin was dependent on the

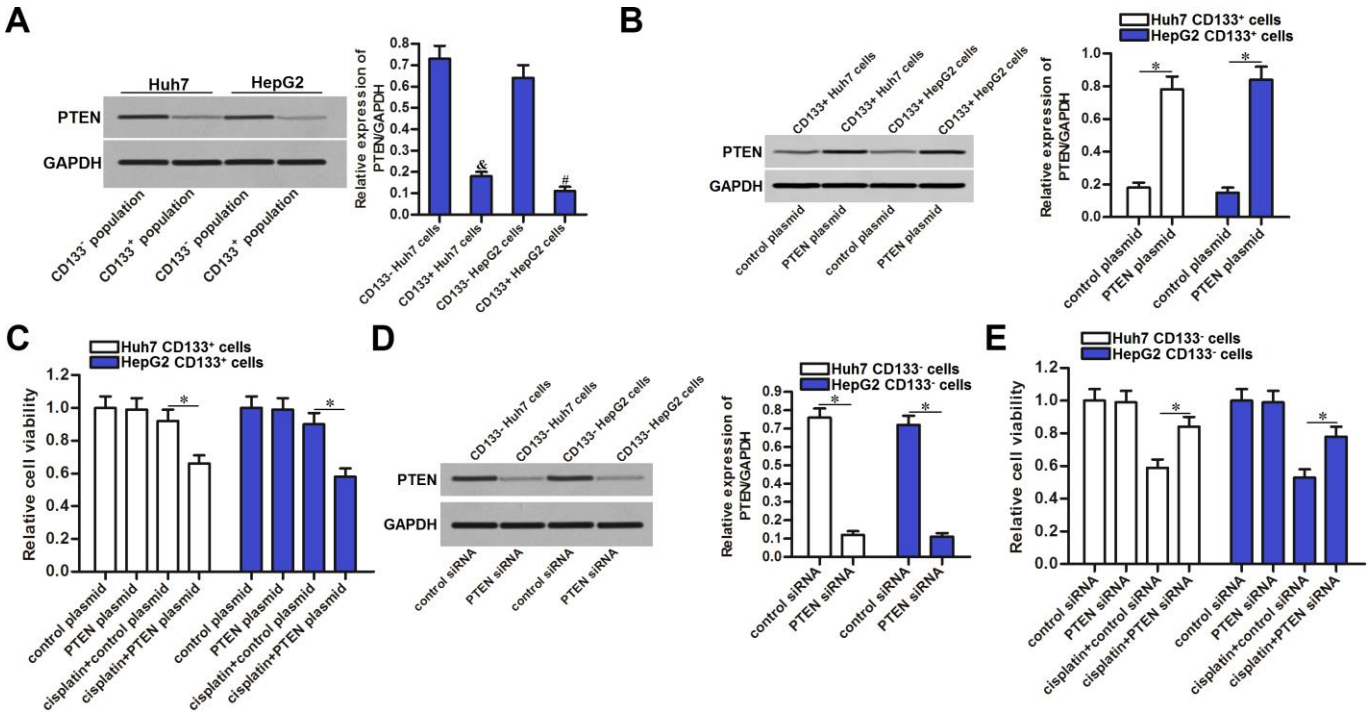

Figure 2. Effect of PTEN on regulating the cisplatin sensitivity of $CD133^+$ and $CD133^-$ HCC cells. (**A**) expression of PTEN in $CD133^+$ and $CD133^-$ Huh7 and HepG2 cells. $^{\&}P<0.05$ *vs.* $CD133^-$ Huh7 cells, $^{\#}P<0.05$ *vs.* $CD133^-$ HepG2 cells. (**B**) Transfection with PTEN plasmid increased the expression of PTEN in $CD133^+$ Huh7 and HepG2 cells. $^*P<0.05$. (**C**) Transfection with PTEN plasmid increased the sensitivity of $CD133^+$ Huh7 and HepG2 cells to cisplatin (5 μM) treatment. $^*P<0.05$. (**D**) Transfection with PTEN siRNA decreased the expression of PTEN in $CD133^-$ Huh7 and HepG2 cells. $^*P<0.05$. (**E**) Transfection with PTEN siRNA decreased the sensitivity of $CD133^-$ Huh7 and HepG2 cells to cisplatin (5 μM) treatment. $^*P<0.05$.

upregulation of PTEN, we knocked down the PTEN in CD133$^+$ Huh7 and HepG2 cells by using PTEN siRNA (Figure 4B). Results of CCK-8 assays showed that treatment with osthole significantly increased the cytotoxicity of cisplatin against CD133$^+$ Huh7 and HepG2 cells (P<0.05). However, knockdown of PTEN abolished the effect of osthole (P<0.05) (Figure 4C). Moreover, results of flow cytometry showed that CD133$^+$ Huh7 and HepG2 cells were resistant to cisplatin-induced apoptosis. However, osthole resensitized the cisplatin-induced apoptosis (P<0.05). On the other hand, transfection with PTEN siRNA inhibited the apoptosis induced by the combination treatment with cisplatin and osthole (P<0.05) (Figure 4D). Taken together, these results indicated that osthole partially reversed the resistance of CD133 positive HCC cells to cisplatin-induced apoptosis through upregulation of PTEN.

Osthole sensitized the cisplatin-induced apoptosis through the PTEN/AKT/Bad/Bcl-2 pathway

Previous study has reported that inhibition of PTEN leads to phosphorylation of AKT [27]. We thus evaluated the role of AKT in CD133$^+$ HCC cells. Results of western blot analysis showed that osthole treatment can reduce the level of phosphorylated AKT (p-AKT) no matter whether the CD133$^+$ Huh7 and HepG2 cells were treated with cisplatin or not. However, knockdown of PTEN was found to abolish the effect of osthole on inhibiting the AKT phosphorylation (Figure 5A). It indicated that osthole treatment reduced the phosphorylation of AKT through the PTEN pathway. Bad, a pro-apoptotic protein, is one of the substrates for AKT [28]. We next found that osthole treatment inhibited the phosphorylation of Bad through increase of PTEN expression (Figure 5A). As osthole decreased the phosphorylation of Bad, results of immunoprecipitation (IP) showed that osthole treatment enhanced the heterodimerization of Bad and Bcl-2 in CD133$^+$ Huh7 and HepG2 cells (Figure 5B). As a result, osthole inactivated the Bcl-2 which is the key anti-apoptotic protein through the PTEN/AKT/Bad pathway. To evaluate the function of mitochondria, we next tested the mitochondrial membrane potential ($\Delta\Psi_m$) and cytosolic cytochrome c in CD133$^+$ Huh7 and HepG2 cells. Results of flow cytometry showed that

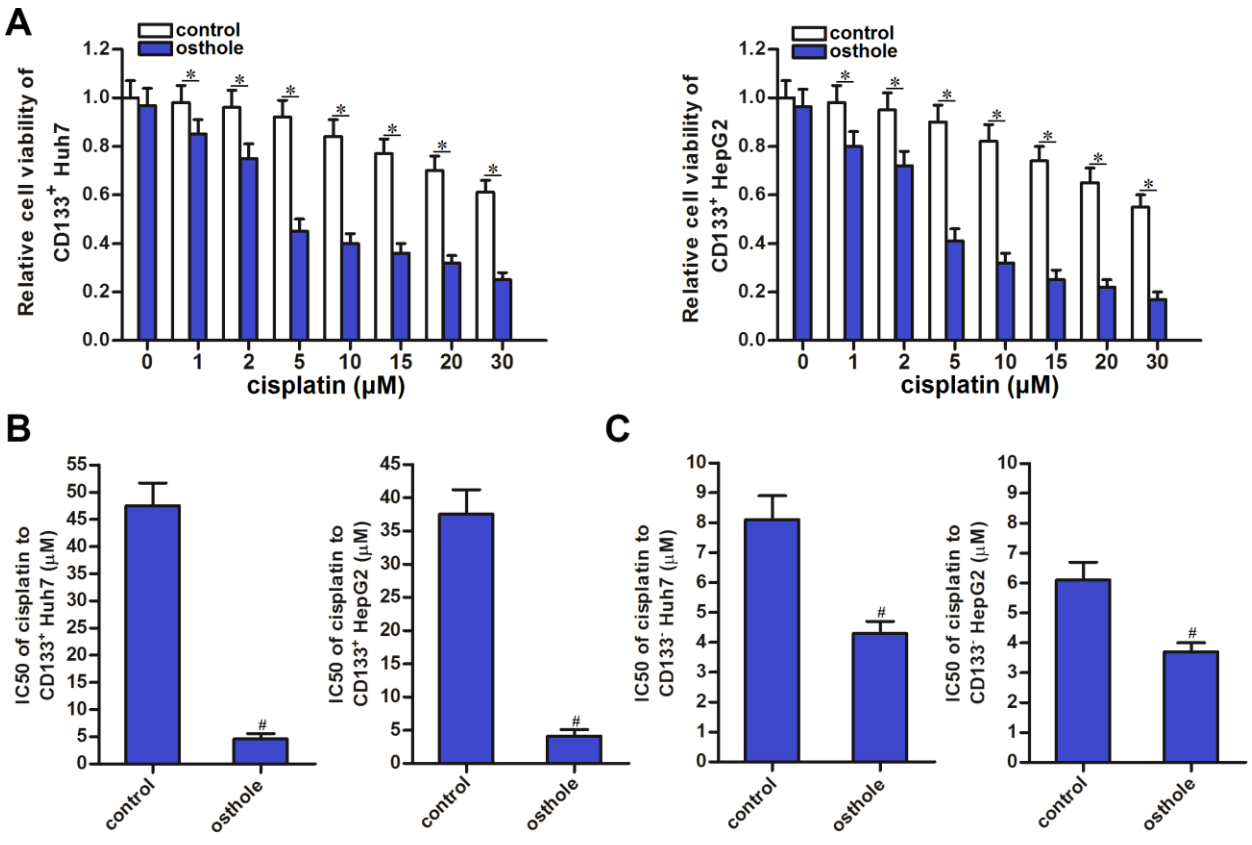

Figure 3. Osthole partially reversed the cisplatin resistance of CD133$^+$ HCC cells. (**A**) Combination treatment with osthole (10 μmol/L) increased the cytotoxicity of cisplatin (0~30 μM) against CD133$^+$ Huh7 and HepG2 cells. *P<0.05. (**B**) Osthole (10 μmol/L) decreased the IC50 of cisplatin to CD133$^+$ Huh7 and HepG2 cells. #P<0.05 *vs.* Control group. (**C**) Effect of osthole (10 μmol/L) on decreasing the IC50 of cisplatin to CD133$^-$ Huh7 and HepG2 cells. #P<0.05 *vs.* Control group.

Table 1. Combination index (CI) with cisplatin and osthole in CD133⁺ Huh7.

Cisplatin single treatment		Osthole single treatment		Combination treatment	Combination index (CI)
Concentration (μM)	Inhibitory rate (%)	Concentration (μM)	Inhibitory rate (%)	Inhibitory rate (%)	
1	2.1	2	3.8	20.4	3.51
2	4.4	4	4.9	32.6	3.59
5	8.7	10	6.3	55.2	3.82
10	16.5	20	8.8	62.8	2.63
15	22.7	30	12.6	67.6	2.08
20	28.8	40	14.5	73.4	1.88
30	37.9	60	16.3	79.5	1.66

Table 2. Combination index (CI) with cisplatin and osthole in CD133⁺ HepG2.

Cisplatin single treatment		Osthole single treatment		Combination treatment	Combination index (CI)
Concentration (μM)	Inhibitory rate (%)	Concentration (μM)	Inhibitory rate (%)	Inhibitory rate (%)	
1	2.4	2	4.0	18.5	2.93
2	5.2	4	4.6	33.2	3.47
5	10.5	10	6.8	59.3	3.58
10	19.4	20	9.4	66.3	2.46
15	26.2	30	14.1	71.7	1.96
20	35.9	40	15.8	77.2	1.68
30	44.7	60	18.4	82.6	1.51

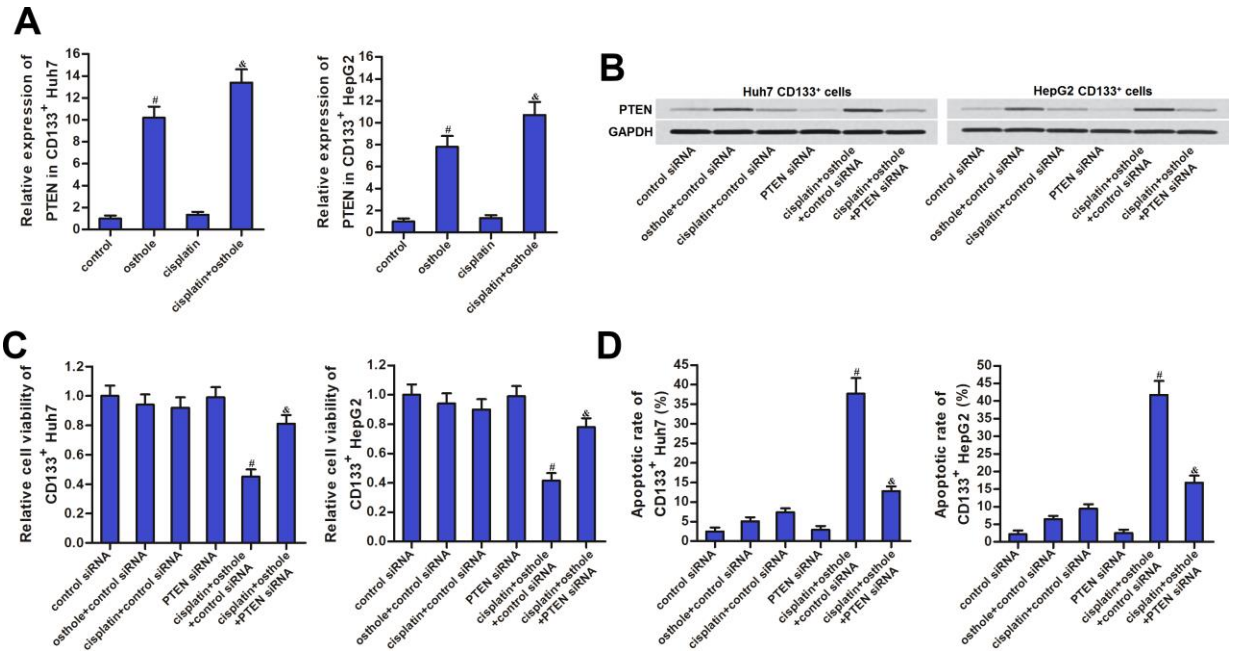

Figure 4. Osthole partially reversed the cisplatin resistance of CD133⁺ HCC cells through the PTEN pathway. (**A**) QRT-PCR analysis was used to test the effect of osthole (10 μmol/L) on changing the expression of PTEN at the mRNA level. #*P*<0.05 *vs.* control group, &*P*<0.05 *vs.* cisplatin group. (**B**) Western blot analysis was used to evaluate the effect of osthole (10 μmol/L) and PTEN siRNA on affecting the expression of PTEN at the protein level. (**C**) Transfection with PTEN siRNA increased the cell viability of CD133⁺ Huh7 and HepG2 cells which were co-treated with osthole (10 μmol/L) and cisplatin (5 μmol/L). #*P*<0.05 *vs.* cisplatin+control siRNA group, &*P*<0.05 *vs.* cisplatin+osthole+control siRNA group. (**D**) Transfection with PTEN siRNA decreased the apoptotic rate of CD133⁺ Huh7 and HepG2 cells which were co-treated with osthole (10 μmol/L) and cisplatin (5 μmol/L). #*P*<0.05 *vs.* cisplatin+control siRNA group, &*P*<0.05 *vs.* cisplatin+osthole+control siRNA group.

combination treatment with osthole enhanced the effect of cisplatin on reducing the $\Delta\Psi_m$ of $CD133^+$ Huh7 and HepG2 cells (Figure 5C). Furthermore, we found the obvious release of cytochrome c in osthole and cisplatin co-treated $CD133^+$ Huh7 and HepG2 cells (Figure 5D). However, transfection with PTEN siRNA abolished the effect of osthole. As the results of mitochondria dysfunction, caspase-9 and caspase-3 were activated in $CD133^+$ Huh7 and HepG2 cells which were co-treated with osthole and cisplatin (Figure 5E). Taken together, we demonstrated that osthole can sensitize the cisplatin-induced apoptosis through the PTEN/AKT/Bad/Bcl-2 pathway in CD133 positive HCC cells.

Osthole attenuated the cisplatin resistance of CD133 positive HCC in vivo

To test the effect of osthole on CD133 positive HCC in vivo, we inoculated the $CD133^+$ Huh7 cells into the nude mice before treatment with osthole and cisplatin. We found that the growth of tumors which were co-treated with osthole and cisplatin was obviously slower than the tumors treated with single cisplatin or osthole (Figure 6A). After euthanasia of nude mice followed by separation of tumor tissues, we observed that the tumors which were co-treated with osthole and cisplatin were smaller and lighter than the tumors treated with single cisplatin or osthole (P<0.05) (Figure 6B, 6C). On the

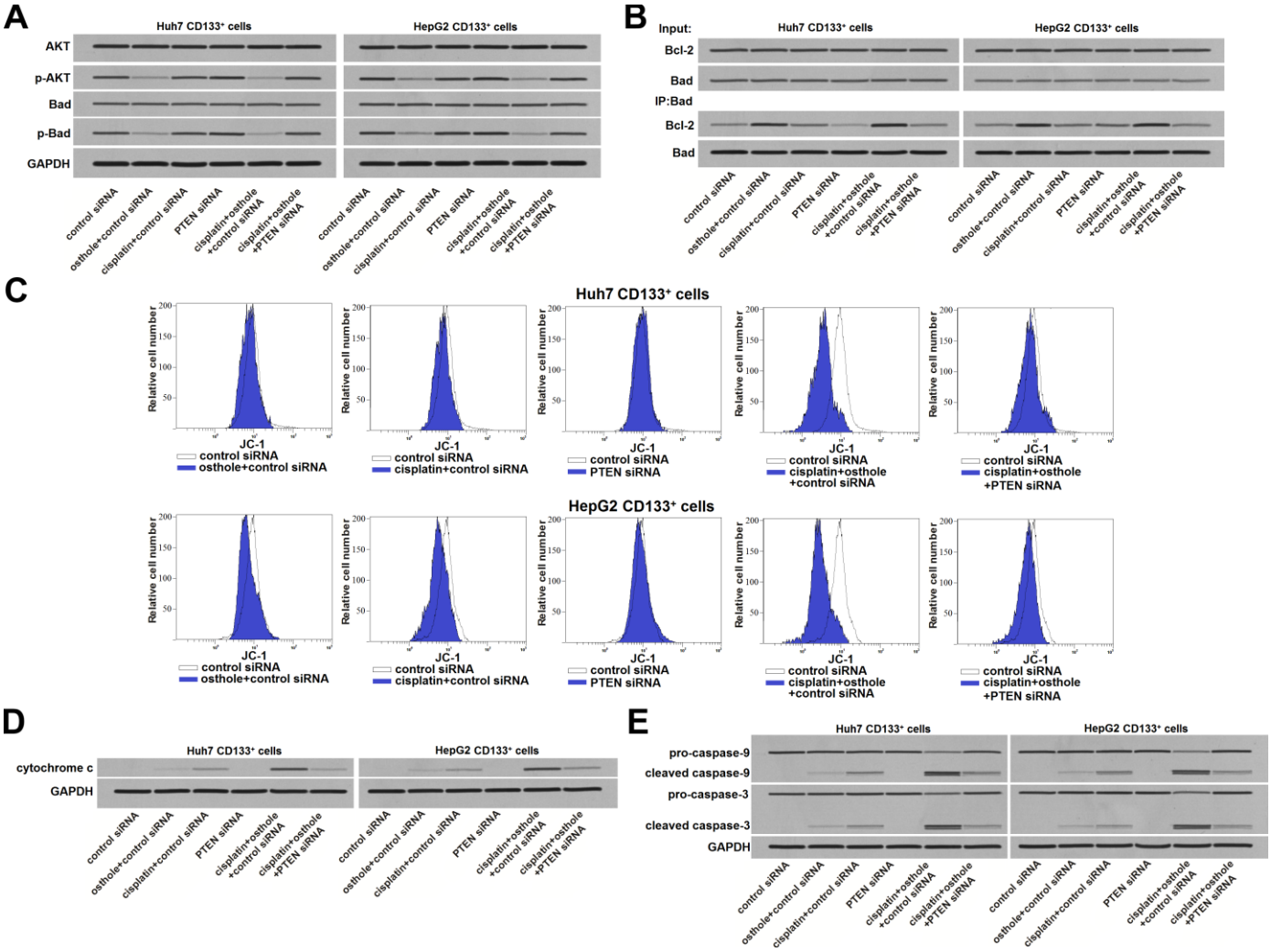

Figure 5. osthole enhanced the cisplatin-induced apoptosis through the PTEN/AKT/Bad/Bcl-2 pathway in $CD133^+$ HCC cells. (**A**) Effect of osthole (10 μmol/L) and PTEN siRNA on affecting the phosphorylation of AKT and Bad in $CD133^+$ Huh7 and HepG2 cells. (**B**) Effect of osthole (10 μmol/L) and PTEN siRNA on affecting the interaction with Bad and Bcl-2 in $CD133^+$ Huh7 and HepG2 cells. (**C**) Osthole (10 μmol/L) enhanced the effect of cisplatin (5 μmol/L) on reducing the mitochondrial membrane potential ($\Delta\Psi_m$) of $CD133^+$ Huh7 and HepG2 cells. (**D**) Osthole (10 μmol/L) increased the cytosolic cytochrome c in $CD133^+$ Huh7 and HepG2 cells which were treated with cisplatin (5 μmol/L). (**E**) Osthole (10 μmol/L) increased the apoptotic rate of $CD133^+$ Huh7 and HepG2 cells which were treated with cisplatin (5 μmol/L).

other hand, results of western blot analysis showed obvious upregulation of PTEN expression in osthole-treated tumors (Figure 6D). Furthermore, we found that osthole enhanced the effect of cisplatin on triggering the caspase-9 and caspase-3 which were the apoptosis markers (Figure 6E). Taken together, These data demonstrated that osthole treatment can attenuate the cisplatin resistance of CD133 positive HCC in vivo.

DISCUSSION

Cisplatin is a platinum-based antineoplastic drug that cross-links with DNA of cancer cells. Subsequently, cisplatin inhibits DNA replication and induces apoptosis of cancer cells [29, 30]. As a broad-spectrum anti-neoplastic drug, cisplatin is commonly used for the treatment of multiple malignant cancers including HCC [31–33]. However, the population of CD133 positive HCC cells showed significant resistance to cisplatin and is responsible for the failure of cisplatin treatment [34]. To improve the curative effect of cisplatin on HCC, CD133 positive cells are important targets. In the present study, we separated the CD133 positive and CD133 negative cells from the HCC cell lines Huh7 and HepG2. We then found that CD133 positive HCC cells exhibited significant cisplatin resistance compared to the CD133 negative HCC cells. It is urgent to overcome the drug resistance of CD133 positive HCC cells.

Studies have reported that multiple natural drugs can be used as sensitizers in chemotherapy. For instance, imperatorin, a linear furanocoumarin compound extracted from the root of *Angelica dahurica*, has been reported to decrease the cisplatin resistance through

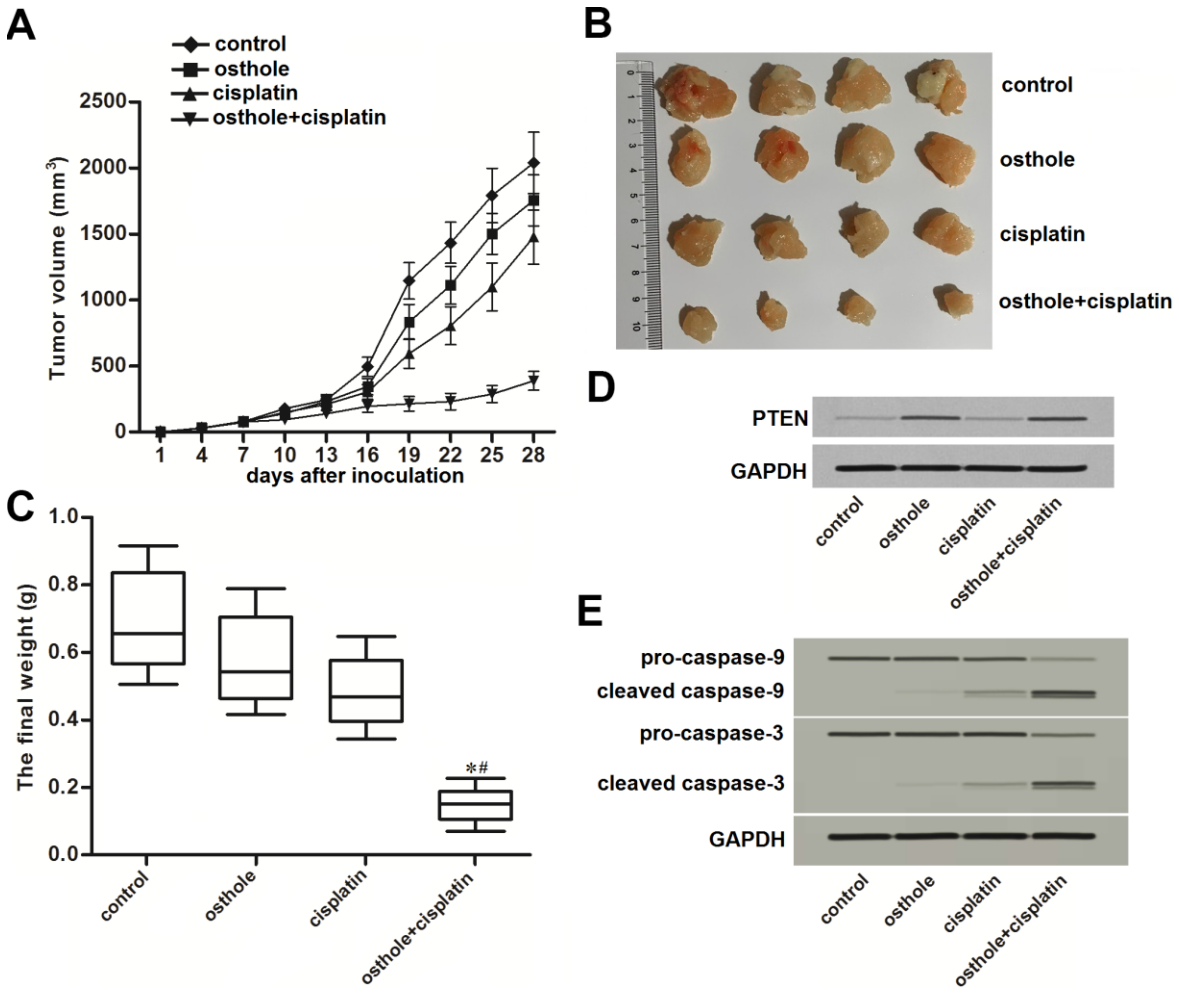

Figure 6. Osthole attenuated the cisplatin resistance of CD133 positive HCC in vivo. (**A**) Growth curve of CD133+ Huh7 originated tumors on nude mice which were treated with cisplatin (8 mg/kg) and osthole (20 mg/kg) twice a week. (**B**) Separated tumor tissues from nude mice after euthanasia. (**C**) The final weight of separated tumor tissues from nude mice after euthanasia. **P*<0.05 *vs.* osthole treatment group, #*P*<0.05 *vs.* cisplatin treatment group. (**D**) Expression of PTEN in purified tumor tissues was tested by western blot analysis. (**E**) Activation of caspase-9 and caspase-3 in purified tumor tissues was tested by western blot analysis.

suppression of MCL-1 [35]; Quercetin, a flavonoid that widely distributes in plant-based foods, has been found to reverse the resistance of prostate cancer to doxorubicin-based therapy [36]; Resveratrol, a natural polyphenol compound, has been proved to restore the sensitivity of glioma cells to temozolamide through inhibiting the activation of Wnt signaling pathway [37]. As one kind of natural drug, osthole has some anti-tumor activity with low toxicity and little side effects. Furthermore, we found the adjuvant effect of osthole on CD133 positive HCC cells in this study. Our results showed that combination index (CI) with cisplatin and osthole on CD133 positive HCC cells was greater than 1.15. These results indicated that osthole can be used as a sensitizer and had synergistic effect on cisplatin. We proved that treatment with osthole can partially reverse the cisplatin resistance of CD133 positive HCC cells.

Phosphatase and tensin homologue (PTEN) has been reported to act as an important tumor suppressor, because it inhibits tumorigenesis and cancer development. Loss of PTEN accumulates the phosphatidylinositol 3, 4, 5-trisphosphate (PIP3) and thus leads to phosphorylation of AKT. As a result, cells develop uncontrolled cell cycle [38, 39]. In this study, we indicated that the drug resistance of CD133 positive HCC cells was associated with the dysfunction of PTEN/AKT-signaling pathway. Furthermore, our results showed that the CD133 positive HCC cells were more sensitive to osthole than the CD133 negative HCC cells. We explained that the synergistic effect of osthole on cisplatin was dependent on the increase of PTEN expression, and the osthole obviously corrected the absence of PTEN in CD133 positive HCC cells.

BCL2 associated agonist of cell death (Bad) is a key substrate of AKT. Non-phosphorylated Bad inactivates the key anti-apoptotic protein of Bcl-2 through conjugation with it. However, Bad can be phospho-rylated by AKT and then releases the Bcl-2. Free Bcl-2 shows powerful antiapoptotic activity and thus inhibits the apoptosis pathway [40, 41]. In the present study, we found that treatment with the natural drug of osthole can increase the expression of PTEN and thus inhibits the phosphorylation of AKT and Bad in CD133 positive HCC cells. As a result, osthole decreased the free Bcl-2 and obviously promoted the mitochondrial apoptosis induced cisplatin.

CONCLUSIONS

We demonstrated the effect of osthole on partially reversing the cisplatin resistance of CD133 positive HCC cells in vitro and in vivo. Combination treatment with osthole and cisplatin may represent a novel strategy for the treatment of HCC.

MATERIALS AND METHODS

Cell lines

The human HCC cell lines Huh7 and HepG2 were purchased from the Cell Bank of the Type Culture Collection of the Chinese Academy of Sciences (Shanghai, China). Cells were cultured in RPMI-1640 medium (Gibco, Carlsbad, CA, USA) supplemented with 10% fetal bovine serum (Gibco). The cells were cultured at 37°C in a humidified incubator with 5% CO_2. To obtain the $CD133^+$ and $CD133^-$ Huh7 and HepG2 cells, the cultured cells were stained with anti-CD133-FITC antibody (Miltenyi Biotec, Germany) for 20 min at room temperature. The population of $CD133^+$ and $CD133^-$ Huh7 and HepG2 cells were analyzed and sorted by using the fluorescent-activated cell sorting equipment (Beckman Coulter, USA).

Gain-of-function and Loss-of-function of PTEN

To knockdown the gene of phosphatase and tensin homologue (PTEN), PTEN small interfering RNA (PTEN siRNA, Santa Cruz Biotechnology, Santa Cruz, CA, USA) was used. To overexpress PTEN, the PTEN eukaryotic expression plasmid was generated by cloning the open reading frame of the PTEN gene into the pcDNA3.1 plasmid (Life Technologies, Carlsbad, CA, USA). For transfection, cells were plated at 30-50% confluence. 24 h later, 50 pmol/ml RNA oligonucleotides or 2 μg/mL plasmids were transfected by using the Lipofectamine™ 2000 reagent (Invitrogen, Carlsbad, CA, USA) according to the manufacturer's instruction.

Quantitative real-time polymerase chain reaction (qRT-PCR)

Total RNA was extracted from cell lines by using Trizol reagent (Thermo Fisher Scientific, Inc., Waltham, MA, USA). cDNA was synthesized by using M-MLV Reverse Transcriptase (Thermo Fisher Scientific, Inc.) following the manufacturer's instruction. Polymerase chain reaction was performed by using a standard protocol from the SYBR Green PCR kit (TaKaRa, Dalian, China). GAPDH gene was used as the internal reference to determine the relative expression of PTEN through the $2^{-\Delta\Delta CT}$ method.

Cell viability assay

Transfected cells were seeded into 96-well culture plates at a density of 5,000 cells/well overnight. Cells were then treated with osthole (10 μmol/L) (Sigma-Aldrich, St. Louis, MO, USA) and different concentrations of cisplatin (0~30 μmol/L) (Sigma-Aldrich) for 48 h. Subsequently, CCK-8 (10 μl) (Beyotime, Shanghai,

China) was added to each well and incubated for 2 h at 37°C. The absorbance of the plates was measured at 450 nm by using a microplate reader (Bio-Tek Instruments, Inc., Norcross, GA, USA). Half maximal inhibitory concentration (IC50) of cisplatin was calculated according to the cell viability curve. Combination index (CI) with cisplatin and osthole was calculated via the following formula: CI=E(A+B)/(EA+EB-EA×EB). EA represents as the inhibitory rate caused by cisplatin; EB represents as the inhibitory rate caused by osthole; E(A+B) represents as the inhibitory rate caused by Combination treatment with cisplatin and osthole. It is considered as simple addition of the two drugs when CI ranges from 0.85 to 1.15; It is considered as simple addition of the two drugs when CI ranges from 0.85 to 1.15; It is considered as the synergistic effect of the two drugs when CI is greater than 1.15; It is considered as the antagonistic effect of the two drugs when CI is less than 0.85.

Immunoprecipitation

Cells were lysed in NP-40 buffer (Beyotime) and centrifuged at 12000g for 10 min. The resulting supernatants were incubated with primary antibody of Bad (Santa Cruz) overnight at 4 ℃. Subsequently, supernatants were incubated with Protein A/G PLUS-Agarose (Santa Cruz) for 2 h. Next, the resulting supernatants were washed with cold NP-40 buffer. The co-precipitated proteins were removed from the agarose beads by boiling in sodium dodecyl sulfate (SDS) sample buffer.

Western blot analysis

Total protein was extracted from cell samples by using RIPA buffer (Beyotime). 50 μg of the extracted and the co-precipitated proteins were separated by 10 % sodium dodecyl sulfate polyacrylamide gel electrophoresis (SDS-PAGE) and transferred to a PVDF membrane (Millipore, Billerica, MA, USA). After blocking in 5% nonfat milk for 2 h at room temperature, the membranes were incubated with anti-p-Bad (1:200, Santa Cruz), anti-p-AKT (1:200, Santa Cruz), anti-PTEN (1:200, Santa Cruz), anti-Bad (1:200, Santa Cruz), anti-AKT (1:200, Santa Cruz), anti-Bcl-2 (1:200, Santa Cruz), anti-cytochrome c (1:200, Santa Cruz), anti-caspase-9 (1:200, Santa Cruz) and anti-caspase-3 (1:200, Santa Cruz). After incubation with primary antibodies, membranes were washed and incubated with a horseradish peroxidase-conjugated secondary antibody (Santa Cruz) for 2 h at room temperature. Proteins on the membrane were visualized by using an enhanced chemiluminescence detection kit (Pierce, Rockford, IL, USA). Glyceraldehyde-3-phosphate (GAPDH) was used as an internal control to ensure equal protein loading. Mitochondria/Cytosol Fraction Kit (BioVision, Milpitas, CA, USA) was used to separate the mitochondria fraction and cytosol fraction before detection of cytochrome c.

Mitochondrial membrane potential ($\Delta\Psi_m$) and cell apoptosis

For detection of mitochondrial membrane potential ($\Delta\Psi_m$), cells were collected and washed with PBS. Subsequently, cells were stained with 5,5′,6,6′-tetrachloro-1,1′,3,3′-tetraethyl imidacarbo cyanine iodide (JC-1, Molecular Probes, Carlsbad, CA, USA) in a 5% CO_2 incubator at 37 °C for 20 min away from light. The samples were then analyzed by flow cytometry. Cells emitting red fluorescence were considered as cells with high $\Delta\Psi_m$. For measurement of cell apoptotic rate, cells were collected and washed with PBS. Subsequently, Annexin V-FITC Apoptosis Detection Kit (Sigma-Aldrich) was used to measure the apoptotic rate.

In vivo experiment

CD133 positive Huh7 cells were inoculated subcutaneously into the BALB/c nude mice (Shanghai Super-B&K Laboratory Animal Corp., Ltd., Shanghai, China). Cisplatin (8 mg/kg) and osthole (20 mg/kg) were administrated by intraperitoneal injection twice a week after xenografts reached 0.5 cm in diameter. Tumor size was measured every three days. Animals were killed 28 days post-injection. The animal care and experimental protocols were approved by the Animal Care Committee of The First Hospital, Jilin University.

Statistical analysis

All data are represented as the mean ± standard deviation (SD) and carried out by at least three independent experiments. Differences between two groups were analyzed by two-tailed Student's *t*-tests. Differences among multiple groups were analyzed by one-way analysis of variance and Bonferroni's *post hoc* test. Statistical analysis was performed by using SPSS 15.0 software (SPSS Inc., Chicago, IL, USA). $P < 0.05$ was considered to be statistically significant.

CONFLICTS OF INTEREST

The authors have no conflicts of interest to declare.

FUNDING

This study is supported by the Wu Jieping Medical Foundation (grant no. 320.6750.17217).

REFERENCES

1. Siegel R, Ma J, Zou Z, Jemal A. Cancer statistics, 2014. CA Cancer J Clin. 2014; 64:9–29. https://doi.org/10.3322/caac.21208 PMID:24399786

2. Ye Y, Song Y, Zhuang J, Wang G, Ni J, Zhang S, Xia W. MicroRNA-302a-3p suppresses hepatocellular carcinoma progression by inhibiting proliferation and invasion. Onco Targets Ther. 2018; 11:8175–84. https://doi.org/10.2147/OTT.S167162 PMID:30573969

3. Liu J, Cui X, Qu L, Hua L, Wu M, Shen Z, Lu C, Ni R. Overexpression of DLX2 is associated with poor prognosis and sorafenib resistance in hepatocellular carcinoma. Exp Mol Pathol. 2016; 101:58–65. https://doi.org/10.1016/j.yexmp.2016.06.003 PMID:27302463

4. Li S, Yang F, Ren X. Immunotherapy for hepatocellular carcinoma. Drug Discov Ther. 2015; 9:363–71. https://doi.org/10.5582/ddt.2015.01054 PMID:26632545

5. Doycheva I, Thuluvath PJ. Systemic therapy for advanced hepatocellular carcinoma: an update of a rapidly evolving field. J Clin Exp Hepatol. 2019; 9:588–96. https://doi.org/10.1016/j.jceh.2019.07.012 PMID:31695249

6. Ikeda M, Morizane C, Ueno M, Okusaka T, Ishii H, Furuse J. Chemotherapy for hepatocellular carcinoma: current status and future perspectives. Jpn J Clin Oncol. 2018; 48:103–14. https://doi.org/10.1093/jjco/hyx180 PMID:29253194

7. Tian N, Shangguan W, Zhou Z, Yao Y, Fan C, Cai L. Lin28b is involved in curcumin-reversed paclitaxel chemoresistance and associated with poor prognosis in hepatocellular carcinoma. J Cancer. 2019; 10:6074–87. https://doi.org/10.7150/jca.33421 PMID:31762817

8. Yin X, Tang B, Li JH, Wang Y, Zhang L, Xie XY, Zhang BH, Qiu SJ, Wu WZ, Ren ZG. ID1 promotes hepatocellular carcinoma proliferation and confers chemoresistance to oxaliplatin by activating pentose phosphate pathway. J Exp Clin Cancer Res. 2017; 36:166. https://doi.org/10.1186/s13046-017-0637-7 PMID:29169374

9. Shang D, Wu J, Guo L, Xu Y, Liu L, Lu J. Metformin increases sensitivity of osteosarcoma stem cells to cisplatin by inhibiting expression of PKM2. Int J Oncol. 2017; 50:1848–56. https://doi.org/10.3892/ijo.2017.3950 PMID:28393220

10. Zhao D, Chen Y, Chen S, Zheng C, Hu J, Luo S. MiR-19a regulates the cell growth and apoptosis of osteosarcoma stem cells by targeting PTEN. Tumour Biol. 2017; 39:1010428317705341. https://doi.org/10.1177/1010428317705341 PMID:28475001

11. Feng X, Jiang J, Shi S, Xie H, Zhou L, Zheng S. Knockdown of miR-25 increases the sensitivity of liver cancer stem cells to TRAIL-induced apoptosis via PTEN/PI3K/Akt/bad signaling pathway. Int J Oncol. 2016; 49:2600–10. https://doi.org/10.3892/ijo.2016.3751 PMID:27840896

12. Shmelkov SV, St Clair R, Lyden D, Rafii S. AC133/CD133/Prominin-1. Int J Biochem Cell Biol. 2005; 37:715–19. https://doi.org/10.1016/j.biocel.2004.08.010 PMID:15694831

13. Liu TJ, Sun BC, Zhao XL, Zhao XM, Sun T, Gu Q, Yao Z, Dong XY, Zhao N, Liu N. CD133+ cells with cancer stem cell characteristics associates with vasculogenic mimicry in triple-negative breast cancer. Oncogene. 2013; 32:544–53. https://doi.org/10.1038/onc.2012.85 PMID:22469978

14. Zhang L, Li H, Ge C, Li M, Zhao FY, Hou HL, Zhu MX, Tian H, Zhang LX, Chen TY, Jiang GP, Xie HY, Cui Y, et al. Inhibitory effects of transcription factor ikaros on the expression of liver cancer stem cell marker CD133 in hepatocellular carcinoma. Oncotarget. 2014; 5:10621–35. https://doi.org/10.18632/oncotarget.2524 PMID:25301737

15. Shackleton M, Quintana E, Fearon ER, Morrison SJ. Heterogeneity in cancer: cancer stem cells versus clonal evolution. Cell. 2009; 138:822–29. https://doi.org/10.1016/j.cell.2009.08.017 PMID:19737509

16. Clarke MF, Fuller M. Stem cells and cancer: two faces of eve. Cell. 2006; 124:1111–15. https://doi.org/10.1016/j.cell.2006.03.011 PMID:16564000

17. Ding K, Liao Y, Gong D, Zhao X, Ji W. Effect of long non-coding RNA H19 on oxidative stress and chemotherapy resistance of CD133+ cancer stem cells via the MAPK/ERK signaling pathway in hepatocellular carcinoma. Biochem Biophys Res Commun. 2018; 502:194–201. https://doi.org/10.1016/j.bbrc.2018.05.143 PMID:29800569

18. Ma S, Lee TK, Zheng BJ, Chan KW, Guan XY. CD133+ HCC cancer stem cells confer chemoresistance by

preferential expression of the Akt/PKB survival pathway. Oncogene. 2008; 27:1749–58. https://doi.org/10.1038/sj.onc.1210811 PMID:17891174

19. Bao R, Shu Y, Wu X, Weng H, Ding Q, Cao Y, Li M, Mu J, Wu W, Ding Q, Tan Z, Liu T, Jiang L, et al. Oridonin induces apoptosis and cell cycle arrest of gallbladder cancer cells via the mitochondrial pathway. BMC Cancer. 2014; 14:217. https://doi.org/10.1186/1471-2407-14-217 PMID:24655726

20. Xiong J, Su T, Qu Z, Yang Q, Wang Y, Li J, Zhou S. Triptolide has anticancer and chemosensitization effects by down-regulating Akt activation through the MDM2/REST pathway in human breast cancer. Oncotarget. 2016; 7:23933–46. https://doi.org/10.18632/oncotarget.8207 PMID:27004407

21. Lin K, Gao Z, Shang B, Sui S, Fu Q. Osthole suppresses the proliferation and accelerates the apoptosis of human glioma cells via the upregulation of microRNA-16 and downregulation of MMP-9. Mol Med Rep. 2015; 12:4592–97. https://doi.org/10.3892/mmr.2015.3929 PMID:26082082

22. Liu J, Zhang W, Zhou L, Wang X, Lian Q. Anti-inflammatory effect and mechanism of osthole in rats. Zhong Yao Cai. 2005; 28:1002–06. PMID:16514888

23. Luszczki JJ, Andres-Mach M, Cisowski W, Mazol I, Glowniak K, Czuczwar SJ. Osthole suppresses seizures in the mouse maximal electroshock seizure model. Eur J Pharmacol. 2009; 607:107–09. https://doi.org/10.1016/j.ejphar.2009.02.022 PMID:19236860

24. Zhang Q, Qin L, He W, Van Puyvelde L, Maes D, Adams A, Zheng H, De Kimpe N. Coumarins from cnidium monnieri and their antiosteoporotic activity. Planta Med. 2007; 73:13–19. https://doi.org/10.1055/s-2006-951724 PMID:17315308

25. Wang L, Peng Y, Shi K, Wang H, Lu J, Li Y, Ma C. Osthole inhibits proliferation of human breast cancer cells by inducing cell cycle arrest and apoptosis. J Biomed Res. 2015; 29:132–38. https://doi.org/10.7555/JBR.27.20120115 PMID:25859268

26. Wen YC, Lee WJ, Tan P, Yang SF, Hsiao M, Lee LM, Chien MH. By inhibiting snail signaling and miR-23a-3p, osthole suppresses the EMT-mediated metastatic ability in prostate cancer. Oncotarget. 2015; 6:21120–36. https://doi.org/10.18632/oncotarget.4229 PMID:26110567

27. Chalhoub N, Baker SJ. PTEN and the PI3-kinase pathway in cancer. Annu Rev Pathol. 2009; 4:127–50. https://doi.org/10.1146/annurev.pathol.4.110807.092311 PMID:18767981

28. Brazil DP, Hemmings BA. Ten years of protein kinase B signalling: a hard Akt to follow. Trends Biochem Sci. 2001; 26:657–64. https://doi.org/10.1016/s0968-0004(01)01958-2 PMID:11701324

29. Zhao JX, Liu H, Lv J, Yang XJ. Wortmannin enhances cisplatin-induced apoptosis in human ovarian cancer cells in vitro. Eur Rev Med Pharmacol Sci. 2014; 18:2428–34. PMID:25268086

30. Xie Q, Wang S, Zhao Y, Zhang Z, Qin C, Yang X. MiR-519d impedes cisplatin-resistance in breast cancer stem cells by down-regulating the expression of MCL-1. Oncotarget. 2017; 8:22003–13. https://doi.org/10.18632/oncotarget.15781 PMID:28423543

31. Ma Y, Zhang NP, An N, Li WY, Zhao W, Liu YC. Clinical efficacy of weekly cisplatin for treatment of patients with breast cancer. Medicine (Baltimore). 2019; 98:e17114. https://doi.org/10.1097/MD.0000000000017114 PMID:31517847

32. Jain A, Jahagirdar D, Nilendu P, Sharma NK. Molecular approaches to potentiate cisplatin responsiveness in carcinoma therapeutics. Expert Rev Anticancer Ther. 2017; 17:815–25. https://doi.org/10.1080/14737140.2017.1356231 PMID:28705091

33. Sheng J, Shen L, Sun L, Zhang X, Cui R, Wang L. Inhibition of PI3K/mTOR increased the sensitivity of hepatocellular carcinoma cells to cisplatin via interference with mitochondrial-lysosomal crosstalk. Cell Prolif. 2019; 52:e12609. https://doi.org/10.1111/cpr.12609 PMID:31033054

34. Xu Y, Lai Y, Weng H, Tan L, Li Y, Chen G, Luo X, Ye Y. MiR-124 sensitizes cisplatin-induced cytotoxicity against $CD133^+$ hepatocellular carcinoma cells by targeting SIRT1/ROS/JNK pathway. Aging (Albany NY). 2019; 11:2551–64. https://doi.org/10.18632/aging.101876 PMID:31056532

35. Hu J, Xu C, Cheng B, Jin L, Li J, Gong Y, Lin W, Pan Z, Pan C. Imperatorin acts as a cisplatin sensitizer via downregulating mcl-1 expression in HCC chemotherapy. Tumour Biol. 2016; 37:331–39.

https://doi.org/10.1007/s13277-015-3591-z
PMID:26219890

36. Shu Y, Xie B, Liang Z, Chen J. Quercetin reverses the doxorubicin resistance of prostate cancer cells by downregulating the expression of c-met. Oncol Lett. 2018; 15:2252–58.
https://doi.org/10.3892/ol.2017.7561
PMID:29434932

37. Yang HC, Wang JY, Bu XY, Yang B, Wang BQ, Hu S, Yan ZY, Gao YS, Han SY, Qu MQ. Resveratrol restores sensitivity of glioma cells to temozolamide through inhibiting the activation of Wnt signaling pathway. J Cell Physiol. 2019; 234:6783–800.
https://doi.org/10.1002/jcp.27409
PMID:30317578

38. Wang YS, Wang YH, Xia HP, Zhou SW, Schmid-Bindert G, Zhou CC. MicroRNA-214 regulates the acquired resistance to gefitinib via the PTEN/AKT pathway in EGFR-mutant cell lines. Asian Pac J Cancer Prev. 2012; 13:255–60.
https://doi.org/10.7314/apjcp.2012.13.1.255
PMID:22502680

39. Darido C, Georgy SR, Wilanowski T, Dworkin S, Auden A, Zhao Q, Rank G, Srivastava S, Finlay MJ, Papenfuss AT, Pandolfi PP, Pearson RB, Jane SM. Targeting of the tumor suppressor GRHL3 by a miR-21-dependent proto-oncogenic network results in PTEN loss and tumorigenesis. Cancer Cell. 2011; 20:635–48.
https://doi.org/10.1016/j.ccr.2011.10.014
PMID:22094257

40. Datta SR, Brunet A, Greenberg ME. Cellular survival: a play in three Akts. Genes Dev. 1999; 13:2905–27.
https://doi.org/10.1101/gad.13.22.2905
PMID:10579998

41. Datta SR, Dudek H, Tao X, Masters S, Fu H, Gotoh Y, Greenberg ME. Akt phosphorylation of BAD couples survival signals to the cell-intrinsic death machinery. Cell. 1997; 91:231–41.
https://doi.org/10.1016/s0092-8674(00)80405-5
PMID:9346240